

Scale invariance in integrable quantum oscillators' long-time dynamics

Emanuele G. Dalla Torre

*Department of Physics and Center for Quantum Entanglement Science
and Technology, Bar-Ilan University, 52900 Ramat Gan, Israel*

Scale invariance usually occurs in extended systems where correlation functions decay algebraically in space and/or time. Here we introduce a new type of scale invariance, occurring in distribution functions of physical observables. At equilibrium, these functions decay over a typical scale set by the temperature, but they can become scale invariant in a sudden quantum quench. We exemplify this effect through the analysis of an integrable quantum oscillator, and show that the associated critical exponent is universal. Our study opens the possibility to address integrability and its breaking in distribution functions, and has immediate applications to matter-wave interferometers.

Introduction Scale invariance is one of the key tools to classify and understand complex systems. For instance, scale invariant critical points can be used to find the universal properties of equilibrium phase transitions through the renormalization group (RG) method. This approach has been recently extended to quantum systems out-of-equilibrium [1–10]. It was found that in the long-time limit, these systems generically tend to equilibrium fixed points, characterized by a finite low-frequency effective temperature. With respect to a quantum critical point, temperature is always a relevant parameter, meaning that it destroys the scale invariance.

Integrable systems offer an exception to this rule because, by construction, they do not thermalize [11]. Finding scale invariant points for integrable systems will allow us to study systems that are close to integrability, giving rise to interesting non-thermal or pre-thermal states [12–17]. The major difficulty is that the spatial correlations of integrable systems are determined by the initial state and are generically not scale invariant. Here we propose a distinct type of scale invariance for integrable quantum systems, which can act as the starting point for a RG analysis of these systems. Our study is based on the observation of scale invariance in the long-time distribution functions of quantum systems that are initially prepared in a pure state.

We specifically focus on the dynamics of a quantum oscillator and demonstrate that its time-averaged distribution probability shows a universal logarithmic divergence close to the classical stable points of the model. At an intuitive level, the scale invariance can be simply understood by considering the linearized equations of motion close to the stable point. Being linear, these equations are invariant under a scaling transformation $x \rightarrow \lambda x$, where λ is some constant. To obtain a scale invariant ensemble, it is then sufficient to complement these equations with a scale invariant initial state, such as a momentum state, whose wavefunction is constant in real space. The key result of this letter is that this simple phenomenon survives non linearities and is intimately related to the model's integrability.

The harmonic oscillator We open our discussion with the analysis of an isolated harmonic oscillator $H_0 = 1/2(x^2 + p^2)$, where x and p are canonical conjugates.

Here the simplest example of a scale invariant state is offered by $|p = 0\rangle$, which satisfies $\langle x|p = 0\rangle = \text{const}$. In a semiclassical description (which is exact for an harmonic oscillator), this state corresponds to the Wigner distribution $P(x, p) = P_0\delta(p)$, where P_0 is a normalization constant. Under the effects of H_0 , this ensemble rotates in phase space: each point follows a circular trajectory around the stable point $x = p = 0$, with constant angular velocity. Thus, after time averaging, one obtains a distribution function that is inversely proportional to the circumference of the circle, or

$$P(x, p) = \frac{A}{\sqrt{x^2 + p^2}}. \quad (1)$$

The relation between A and P_0 can be determined by demanding the conservation of probability over a circle of radius R , $\int_{-R}^R dx P_0 = \int_{x^2+p^2 < R^2} dp dx P(x, p)$. Here the LHS and RHS are respectively the integrated probabilities in the initial state and in the time-averaged distributions. The latter integral can be easily solved using polar coordinates, leading to $2RP_0 = 2\pi RA$, or $A = P_0/\pi$.

We can now use Eq. (1) to compute the (time-averaged) marginal probability

$$\begin{aligned} P(x) &= \int_{-R}^R dp P(x, p) = \frac{P_0}{\pi} \int_{-R}^R dp \frac{1}{\sqrt{x^2 + p^2}} \\ &= \frac{2P_0}{\pi} \text{arsh} \left(\frac{R}{|x|} \right) \xrightarrow{x \rightarrow 0} -\frac{2P_0}{\pi} \log(|x|). \end{aligned} \quad (2)$$

We find that the distribution function of x diverges logarithmically around $x = 0$. A similar argument is valid for the marginal distribution of p , as well as linear superpositions of x and p . Note that the logarithmic divergence does not pose any problem in terms of normalizability: $\int_0^1 dx \log(x)$ is finite.

Eq. (2) is universal in the sense that it does not depend on the microscopic details of the Hamiltonian: As long as the stability of the $x = p = 0$ point is preserved, the dynamics in its surroundings is characterized by invariant tori. For a scale invariant initial state, the time-averaged $P(x, p)$ is inversely proportional to the circumference of the appropriate torus, which is in turn proportional to the distance from the stable point. The integration over

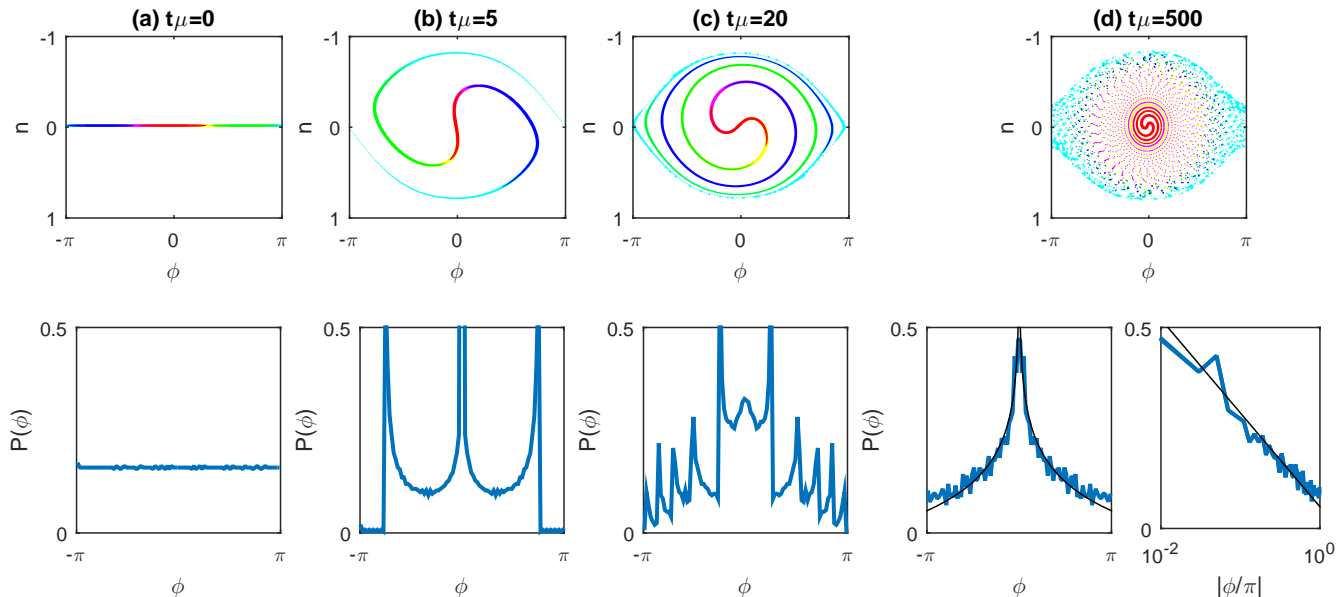


FIG. 1. Upper panel: Phase-space representation of the time evolution of a quantum oscillator (5), obtained by the numerical solution of Eq. (5) with $g = 0.2$. Each plot represents the dynamics of 4000 points with initial conditions $n(t=0) = 2000$ and $\phi(t=0)$ uniformly distributed between $-\pi$ and π . Each pixel is colored according to the corresponding value of $\phi(t=0)$. (a) The initial state is $|n=0\rangle$ and corresponds to a thin vertical line in phase space. (b-d) Time snapshots of the evolution of the quantum ensemble. Lower panel: Time evolution of the marginal probability distribution $P(\phi(t))$. At long times $P(\phi) \approx -1/\pi^2 \log(|\phi|) + 0.17$ (black line).

one variable will then generically lead to a logarithmic divergence, whose prefactor is solely determined by the normalization of the initial conditions. Furthermore, as we will see, in the presence of nonlinearities, the periods of the different trajectories are unequal, and the long-time probability distribution will generically tend to the time-averaged expression.

A nonlinear quantum oscillator To exemplify this effect, we focus on the two-site Hubbard model

$$H = \frac{\mu}{N} \sum_{i=1,2} \left(\psi_i^\dagger \psi_i - \frac{N}{2} \right)^2 + J(\psi_1^\dagger \psi_2 + h.c.), \quad (3)$$

with chemical potential μ , tunneling element J , and a total number of particles $\psi_1^\dagger \psi_1 + \psi_2^\dagger \psi_2 = N$. The equilibrium and nonequilibrium properties of this Hamiltonian have been thoroughly theoretically described (see for example Refs. [18–24]) and experimentally realized with exciton polaritons [25, 26] and trapped ions [27], and ultracold atoms [28–30]. For these latter systems, the observation of full distribution probabilities is a standard tool matter-wave interferometry [31–35].

The Hamiltonian (3) is conveniently described in terms of N spin-1/2 variables, $\vec{\sigma}_i$, whose z component describes the site occupied by the i^{th} particle [36, 37][38]. By introducing the total spin operator $\vec{S} = \sum_{i=1}^N \vec{\sigma}_i$, one can exactly map Eq. (3) to the Lipkin-Meshkov-Glick nonlinear quantum oscillator [39]

$$H = \frac{\mu}{S} S_z^2 + 2JS_x. \quad (4)$$

Here the spin operators \vec{S} satisfy $[S_x, S_y] = iS_z$ and $S_x^2 + S_y^2 + S_z^2 = S(S+1)$, with $S = N/2$. For large S , the Hamiltonian (4) is well approximated by a semiclassical description [40, 41], where the spin operators are substituted by two continuous variables, n and ϕ , defined by $S_z/S = n$, $S_\pm/S = \sqrt{1-n^2} \exp(\pm i\phi)/2$. The canonical variables n and ϕ respectively correspond to the number and phase differences of the two-site Bose-Hubbard model (3). Under this transformation, the Hamiltonian (4) is mapped to

$$\frac{H}{2S} = \frac{\mu}{2} n^2 + J\sqrt{1-n^2} \cos(\phi). \quad (5)$$

The classical dynamics associated with the Hamiltonian (5) has two fixed points on the line $n=0$, respectively at $\phi=0$ and $\phi=\pi$ [42]. Their dynamical stability depends on the ratio $\Gamma = J/\mu$: for $\Gamma < 1$, the system is stable only around $\phi=0$, while for $\Gamma > 1$ the system becomes stable around $\phi=\pi$ as well. This transition is associated with the disappearance of macroscopic self-trapping [43, 44]. In a model with negative μ (such as a mean-field ferromagnet), the point $\Gamma=1$ corresponds to an equilibrium phase transition with order parameter $\langle S_z \rangle$. As we will see, the scaling exponent of the time-averaged distribution function is discontinuous at this transition as well.

To achieve a scale invariant distribution function we consider the initial states $|S_z=0\rangle$. This state corresponds to the ground state of the Hamiltonians (3) and (4) with $J=0$. Thus, the present dynamics is equivalent to the experimentally-relevant situation of a quantum quench in which J is suddenly changed from 0 to a

finite value [45, 46]. In the semiclassical description of Eq. (5), this state is mapped to an ensemble with $n = 0$ and a uniformly distributed $\phi \in (-\pi, \pi)$, or equivalently $P(n, \phi) = \delta(n)/2\pi$. Fig. 1 shows the evolution of this ensemble, obtained by the numerical solution of the classical equations of motion associated with the Hamiltonian (5). The marginal distribution $P(\phi)$ is shown in the lower panel and evolves from $P(\phi) = 1/2\pi$ to the universal shape $P(\phi) = -1/\pi^2 \log(\phi)$, as predicted by Eq. (2). This result shows that the nonlinear terms present in the Hamiltonian (5) do not affect the logarithmic divergence close to the stable point. This finding can be reformulated in an RG logic: The nonlinear terms tend to decrease under the scaling transformation $x \rightarrow \lambda x$. They are therefore irrelevant in an RG sense and do not affect the universal critical exponent $1/\pi^2$.

Full quantum evolution We now compare the above-mentioned semiclassical calculations to the results obtained through the exact diagonalization of the quantum Hamiltonian (4). This Hamiltonian conserves the total spin S^2 , leading to a reduced Hilbert space of size $2S + 1$. Thanks to this simplification, we can exactly diagonalize the model for relatively large $S \sim 1000$.

Based on the previous semiclassical analysis we expect to observe a logarithmic divergence in the distribution of the operator $m_y \equiv S_y/S = \sqrt{1-n^2} \sin(\phi)$, which can be approximated by $m_y \approx \phi$ close to the fixed points. The time-averaged distribution function of m_y is defined quantum mechanically by

$$P(m_y) = \lim_{T \rightarrow \infty} \frac{1}{T} \int_0^T dt |\langle S_y = m_y S | \psi(t) \rangle|^2, \quad (6)$$

where $|\psi(t)\rangle = e^{-i\hat{H}t}|S_z = 0\rangle$, and H is the Hamiltonian (4). As shown in Fig. 2, the resulting distribution function diverges logarithmically around $m_y = 0$. Because at $\Gamma = 1$ the number of stable points across the $m_z = 0$ line jumps from 1 to 2, we obtain

$$P(m_y) = -\frac{1}{\pi^2} (1 + \Theta(\Gamma - 1)) \log(m_y). \quad (7)$$

This universal result is in agreement with the numerical findings shown in the inset of Fig. 2. A closer inspection of Fig. 2 shows that for $\Gamma < 1$, $P(m_y)$ shows a cusp at finite m_y . As approaching $\Gamma = 1$, the cusp shifts to smaller m_y and, for $\Gamma > 1$, it joins the divergence at $m_y = 0$, doubling the prefactor of the logarithm [47].

Breaking of integrability We now consider a simple term that breaks integrability, namely dissipation, through the following equations of motion

$$\begin{aligned} \frac{d\phi}{dt} &= n - \Gamma \frac{n}{\sqrt{1-n^2}} \cos(\phi) \\ \frac{dn}{dt} &= -\Gamma \sqrt{1-n^2} \sin(\phi) - 2\eta n. \end{aligned} \quad (8)$$

In the limit of $\eta \rightarrow 0$ these equations are equivalent to the Hamiltonian (5). The numerical solution of Eqs. (8) for

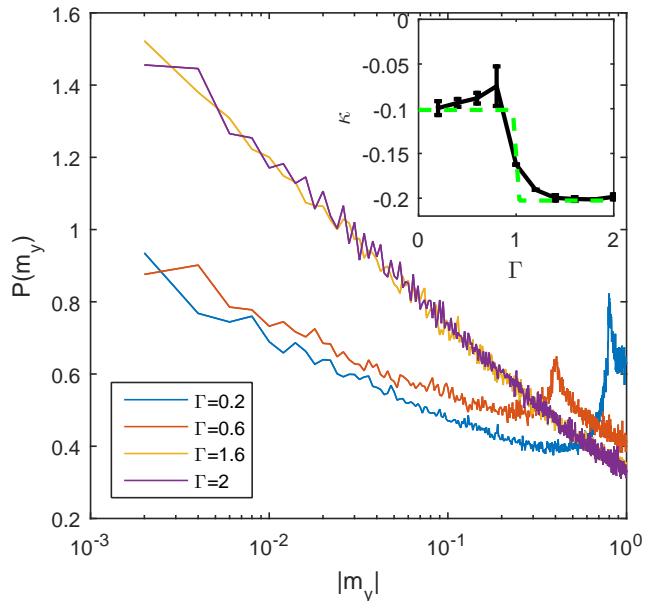


FIG. 2. (a) Time-averaged probability distribution function of $m_y = S_y/S$, defined in Eq.(6) and obtained using the exact diagonalization of the Hamiltonian (4) with $S = 1000$. The distribution functions displays a logarithmic divergence around $m_y = 0$, $P(m_y) \approx \kappa \log(m_y)$. (b) Numerically determined prefactor κ as a function of the normalized tunneling Γ . The numerical findings are consistent with the theoretical prediction of $\kappa = -1/\pi^2$ for $\Gamma < 1$ and $\kappa = -2/\pi^2$ for $\Gamma > 1$.

one specific initial condition ($n(t=0) = 0$, $\phi(t=0) = -0.93\pi$, $J = 0.2$ and $\eta = 0.1$) is shown in Fig. 3(a) and shows a spiral path towards the stable point $n = \phi = 0$.

Interestingly, the dissipation term η is invariant under the scaling transformation $\phi \rightarrow \lambda\phi$, $n \rightarrow \lambda n$. In analogy to the effect of marginal operators on RG flows, it is therefore natural to expect that this term will modify the prefactor of the logarithmic divergence. This hypothesis is confirmed by the numerical calculations shown in Fig. 3. We find that the distributions is still logarithmically divergent (subplot (c)), but the prefactor decreases as a function of time (subplot (d)). To understand this result, it is useful to linearize Eqs. (8), giving rise to the equations of motion of a damped harmonic oscillator. For this model, each point evolves as $x(t) = x_0 e^{-\eta t} \cos(\omega t)$, and the phase-space density grows accordingly as $A(t) = A_0 e^{\eta t}$. The time-averaged joint distribution is then given by an expression analogous to Eq. (1),

$$P_T(x, p) = \frac{1}{T} \int_0^T dt \frac{A(t)}{\sqrt{x^2 + p^2}} = \left(\frac{e^{\eta T} - 1}{\eta T} \right) \frac{A}{\sqrt{x^2 + p^2}}.$$

The distribution function of ϕ can be computed as before, leading to

$$P_T(\phi) = -\frac{1}{\pi^2} \left(\frac{e^{\eta T} - 1}{\eta T} \right) \log(|\phi|) \quad (9)$$

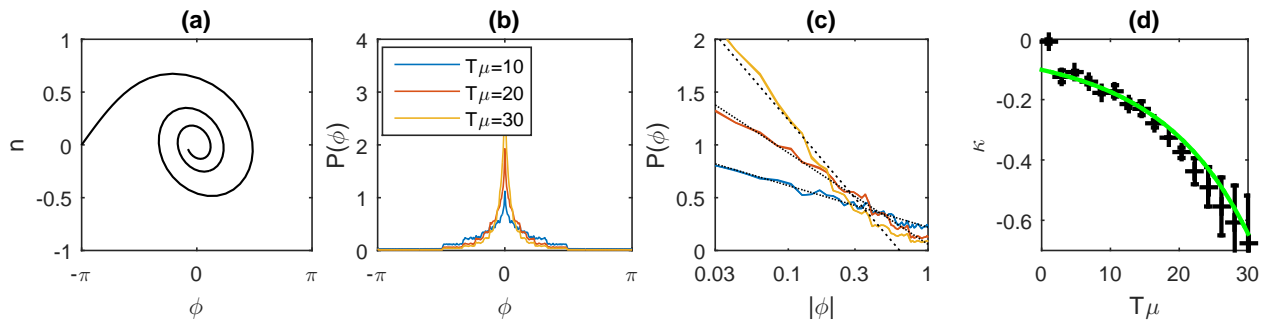


FIG. 3. (a) Phase space of evolution in the presence of dissipation, Eq. (8). (b-c) Time-averaged probability distribution of ϕ for different waiting times T . The initial state corresponds to an ensemble with $n = 0$ and ϕ uniformly distributed on $[-\pi, \pi]$. (d) Prefactor of the logarithm, obtained by a numerical fit of the form $P_T(\phi) = \kappa(t) \log(|\phi|)$ (crosses) and by the analytical expression Eq.(9) (continuous line).

As shown in Fig. 3(b-d) this expression is in quantitative agreement with the numerical solution of the non-linear model.

Conclusion and discussion In summary, we considered the time evolution of nonlinear quantum oscillators with scale invariant initial states (such as momentum states). Close to stable points of the classical dynamics, the evolution is characterized by concentric tori. The time-averaged distribution functions are then inversely proportional to the distance from the stable points, and give rise to logarithmically diverging marginal distribution functions. By considering classical and quantum nonlinear models, we demonstrated the universality of our result and its independence on details of the Hamiltonian. In the presence of a simple integrability breaking term (dissipation), the logarithmic divergence is preserved, but its prefactor becomes time-dependent and non-universal.

In our analysis, we only considered irrelevant and marginal terms, whose dimensions can be inferred by scaling arguments. An important question involves the fate of relevant perturbation, such as external forces. In particular, if the dissipation term η is due to the coupling to an equilibrium bath, random forces are expected to appear as a consequence of the fluctuation-dissipation theorem. These forces give rise to inhomogeneous terms

in Eq. (8) and presumably lead to an equilibrium distribution function, of the form $P_{\text{eq}}(\phi) = \exp(-\beta E(\phi))$, where the $E(\phi)$ is the energy of the oscillator. This expression is generically analytical around $\phi = 0$, indicating that in equilibrium systems $P(\phi)$ does not diverge. Thus, the predicted logarithmic divergence implies the absence of thermalization and can be used as an indicator of integrability.

Thermalization can be prevented by disorder as well, through a phenomenon known as many-body localization (MBL) [48, 49]. MBL systems are effectively integrable because they can be mapped to collections of independent local degrees of freedom [50]. As a consequence, the present analysis still applies, predicting that sudden quenches should lead to logarithmic divergence of the probability distributions. This conjecture offers a possible explanation for the non-Gaussian distribution functions observed numerically in dynamics of MBL systems [51].

Acknowledgment We thank Baruch Barzel, Eugene Demler, Jonathan Karp, Marine Pigneur, Shoumi Roy, Angelo Russomanno, Joerg Schmiedmayer, Thomas Schweigler for many useful discussions. This work was supported by the Israeli Science Foundation Grant No. 1542/14. The author has no competing financial interest.

-
- [1] A. Mitra, S. Takei, Y. B. Kim, and A. Millis, *Physical Review Letters* **97**, 236808 (2006).
[2] S. G. Jakobs, V. Meden, and H. Schoeller, *Physical Review Letters* **99**, 150603 (2007).
[3] E. Dalla Torre, E. Demler, T. Giamarchi, and E. Altman, *Nature Physics* **6**, 806 (2010).
[4] S. Diehl, A. Tomadin, A. Micheli, R. Fazio, and P. Zoller, *Physical Review Letters* **105**, 015702 (2010).
[5] A. Mitra and T. Giamarchi, *Physical Review Letters* **107**, 150602 (2011).
[6] A. Mitra and T. Giamarchi, *Physical Review B* **85**, 075117 (2012).
[7] E. Dalla Torre, E. Demler, T. Giamarchi, and E. Altman, *Physical Review B* **85**, 184302 (2012).
[8] E. Dalla Torre, E. Demler, T. Giamarchi, and E. Altman, *Physica Scripta* **2012**, 014026 (2012).
[9] E. Dalla Torre, S. Diehl, M. D. Lukin, S. Sachdev, and P. Strack, *Physical Review A* **87**, 023831 (2013).
[10] L. Sieberer, S. Huber, E. Altman, and S. Diehl, *Physical Review B* **89**, 134310 (2014).
[11] Among different possible definitions of quantum integrability [52, 53], here we refer to the integrability of their classical counterparts. This definition is known to exclude from the discussion subtle types of integrability, such as

- the Bethe-ansatz integrability, where the present result are indeed not expected to directly apply.
- [12] J. Berges, S. Borsányi, and C. Wetterich, *Physical Review Letters* **93**, 142002 (2004).
- [13] M. Marcuzzi, J. Marino, A. Gambassi, and A. Silva, *Physical review letters* **111**, 197203 (2013).
- [14] F. Essler, S. Kehrein, S. Manmana, and N. Robinson, *Physical Review B* **89**, 165104 (2014).
- [15] B. Bertini, F. H. Essler, S. Groha, and N. J. Robinson, *Physical review letters* **115**, 180601 (2015).
- [16] T. Langen, T. Gasenzer, and J. Schmiedmayer, *arXiv preprint* **1603.09385** (2016).
- [17] N. Yao, C. Laumann, J. I. Cirac, M. Lukin, and J. Moore, *Physical review letters* **117**, 240601 (2016).
- [18] G.-S. Paraoanu, S. Kohler, F. Sols, and A. Leggett, *Journal of Physics B: Atomic, Molecular and Optical Physics* **34**, 4689 (2001).
- [19] A. Foerster, J. Links, and H.-Q. Zhou, *Classical and Quantum Nonlinear Integrable Systems: Theory and Application*, 208 (2003).
- [20] E. Boukobza, M. Chuchem, D. Cohen, and A. Vardi, *Physical review letters* **102**, 180403 (2009).
- [21] C. Bodet, J. Esteve, M. Oberthaler, and T. Gasenzer, *Physical Review A* **81**, 063605 (2010).
- [22] G. Mazza and M. Fabrizio, *Physical Review B* **86**, 184303 (2012).
- [23] H. Veksler and S. Fishman, *New Journal of Physics* **17**, 053030 (2015).
- [24] I. Lovas, J. Fortágh, E. Demler, and G. Zaránd, *ArXiv e-prints* (2017), arXiv:1706.04571 [cond-mat.quant-gas].
- [25] K. G. Lagoudakis, B. Pietka, M. Wouters, R. André, and B. Deveaud-Plédran, *Physical Review Letters* **105**, 120403 (2010).
- [26] M. Abbarchi, A. Amo, V. Sala, D. Solnyshkov, H. Flayac, L. Ferrier, I. Sagnes, E. Galopin, A. Lemaître, G. Malpuech, *et al.*, *Nature Physics* **9**, 275 (2013).
- [27] J. G. Bohnet, B. C. Sawyer, J. W. Britton, M. L. Wall, A. M. Rey, M. Foss-Feig, and J. J. Bollinger, *Science* **352**, 1297 (2016).
- [28] M. Albiez, R. Gati, J. Fölling, S. Hunsmann, M. Cristiani, and M. K. Oberthaler, *Physical review letters* **95**, 010402 (2005).
- [29] T. Schumm, S. Hofferberth, L. M. Andersson, S. Wildermuth, S. Groth, I. Bar-Joseph, J. Schmiedmayer, and P. Krüger, *Nature physics* **1**, 57 (2005).
- [30] S. Trotzky, P. Cheinet, S. Fölling, M. Feld, U. Schnorrberger, A. M. Rey, A. Polkovnikov, E. Demler, M. Lukin, and I. Bloch, *Science* **319**, 295 (2008).
- [31] T. Kitagawa, A. Imambekov, J. Schmiedmayer, and E. Demler, *New Journal of Physics* **13**, 073018 (2011).
- [32] M. Gring, M. Kuhnert, T. Langen, T. Kitagawa, B. Rauer, M. Schreitl, I. Mazets, D. A. Smith, E. Demler, and J. Schmiedmayer, *Science* **337**, 1318 (2012).
- [33] D. A. Smith, M. Gring, T. Langen, M. Kuhnert, B. Rauer, R. Geiger, T. Kitagawa, I. Mazets, E. Demler, and J. Schmiedmayer, *New Journal of Physics* **15**, 075011 (2013).
- [34] T. Schweigler, V. Kasper, S. Erne, I. Mazets, B. Rauer, F. Cataldini, T. Langen, T. Gasenzer, J. Berges, and J. Schmiedmayer, *Nature* **545**, 323 (2017).
- [35] F. Cerisola, Y. Margalit, S. Machluf, A. J. Roncaglia, J. P. Paz, and R. Folman, *ArXiv e-prints* (2017), arXiv:1706.07866 [quant-ph].
- [36] J. Schwinger, *On Angular Momentum*, Tech. Rep. (Harvard Univ.; Nuclear Development Associates, Inc.(US), 1952).
- [37] A. Auerbach, *Interacting electrons and quantum magnetism* (Springer Science & Business Media, 2012).
- [38] Here we refer to the Schwinger boson representation of spin operators $S_\alpha = 1/2 \sum_{i,j=1,2} \hat{\psi}_i^\dagger \sigma_\alpha^{i,j} \hat{\psi}_j$, where $\alpha = x, y, z$ and σ_α are Pauli matrices.
- [39] H. J. Lipkin, N. Meshkov, and A. Glick, *Nuclear Physics* **62**, 188 (1965).
- [40] B. Sciolla and G. Biroli, *Journal of Statistical Mechanics: Theory and Experiment* **2011**, P11003 (2011).
- [41] A. Russmanno, Ph.D. thesis, SISSA (2014).
- [42] In the regime $\Gamma < 1$ the system has two additional stable fixed points at $n = \pm n_0 \neq 0$, which correspond to the two ferromagnetic equilibrium states. The presence of these stable points is at the origin of the macroscopic quantum self-trapping effect. In the present discussion we consider only initial states with $n = 0$, whose dynamics is not directly connected to these stable points.
- [43] S. Raghavan, A. Smerzi, S. Fantoni, and S. Shenoy, *Physical Review A* **59**, 620 (1999).
- [44] R. Hipolito and A. Polkovnikov, *Physical Review A* **81**, 013621 (2010).
- [45] A. Iucci and M. A. Cazalilla, *New Journal of Physics* **12**, 055019 (2010).
- [46] E. Dalla Torre, E. Demler, and A. Polkovnikov, *Physical Review Letters* **110**, 090404 (2013).
- [47] A similar behavior is shown by the numerical solution of the semiclassical equations of motion associated with (5).
- [48] D. Basko, I. Aleiner, and B. Altshuler, *Annals of physics* **321**, 1126 (2006).
- [49] V. Oganessian and D. A. Huse, *Physical Review B* **75**, 155111 (2007).
- [50] A. Chandran, I. H. Kim, G. Vidal, and D. A. Abanin, *Physical Review B* **91**, 085425 (2015).
- [51] D. J. Luitz and Y. Bar Lev, *Physical Review Letters* **117**, 170404 (2016).
- [52] S. Weigert, *Physica D: Nonlinear Phenomena* **56**, 107 (1992).
- [53] J.-S. Caux and J. Mossel, *Journal of Statistical Mechanics: Theory and Experiment* **2011**, P02023 (2011).